Acta Cryst. (1980). A36, 16–21

Two-Dimensional Lattice Images of the Mg-Base Friauf–Laves Phase and a New Type of Defect

BY Y. KITANO, Y. KOMURA AND H. KAJIWARA

Department of Materials Science, Faculty of Science, Hiroshima University, Higashi-senda-machi, Hiroshima 730, *Japan*

AND E. WATANABE

JEOL Ltd., 1418 *Nakagami, Akishima, Tokyo* 196, *Japan*

(*Received* 19 *February* 1979; *accepted* 27 *July* 1979)

Abstract

Two-dimensional lattice images have been obtained for the two-, four-, and nine-layer type structures of the Friauf–Laves phase, $Mg(Cu_{0.535}Al_{0.465})_2$. An intimate correlation is established between the lattice image and the crystal structure. With this relation, layer sequences of disordered stacking regions are determined. A new type of linear defect is found in the images and a structural model of the defect is proposed. The defect is always accompanied by a stacking fault, which is different from the usual stacking faults observed in close-packed structures.

Introduction

The Mg-base pseudo-binary Friauf–Laves phases have been extensively investigated in our laboratory (Komura, 1962; Komura, Mitarai, Nakatani, Iba & Shimizu, 1970; Komura, Mitarai, Nakaue & Tsujimoto, 1972; Komura & Kitano, 1977), and several stacking variants were found in addition to three fundamental structures of C_{14}($MgZn_2$-type), C_{15}($MgCu_2$-type) and C_{36}($MgNi_2$-type). In a previous paper (Kitano, Komura & Kajiwara, 1977), an electron microscope observation (JEM 200A) of a Friauf–Laves phase $Mg(Cu_{1-x}Al_x)_2$ with $x = 0{\cdot}465$ was reported, and one-dimensional lattice images of the polytypic structures, two-, four-, six-, nine-, ten- and 16-layer type structures were presented. A remarkable correspondence was found between the lattice image and the layer sequence. The lattice images consist of bright and dark fringes with narrow and wide bands. Every bright narrow fringe is attributed to one of A, B and C layers and a bright wide one to two successive such layers. Every dark narrow fringe is attributed to one of A', B' and C' layers, and a dark wide one to two successive such layers. Here A, B, C and A', B', C' represent the six kinds of compound layers of the Friauf–Laves phase, which is shown below. From the correspondence, we can easily draw an inference on a stacking sequence of unknown structures.

The purpose of the present paper is to represent two-dimensional lattice images of the $Mg(Cu_{1-x}Al_x)_2$ with $x = 0{\cdot}465$, observed with a high-resolution electron microscope (JEM 100C). The specimen is the same as in the previous paper (Kitano, Komura & Kajiwara, 1977). In order to improve the resolution, as many scattered waves as possible were used to form the images. An intimate correlation will also be shown between the two-dimensional image and the structure. The image shows an array of white patches. Relative shifts of the white patches parallel to the layer plane are found to correspond to the shifts of successive layers of A, B, C or A', B', C'. This correlation also enables us to determine the stacking sequence of the specimen from the lattice image, even the layer stacking sequence is not regular. The lattice images frequently exhibit a new type of defect, which has a characteristic atomic arrangement and is always accompanied by a stacking fault.

Structure of the Friauf–Laves phase

The structures of the Friauf–Laves phase can be described in terms of the stacking sequence of six compound layers; A, A', B, B', C and C' (Komura, 1962), here the A or A' layer (Fig. 1) is composed of a kagomé net (Frank & Kasper, 1959) and three triangular nets. Cu and Al atoms form the kagomé net at $z = 0$, and Mg atoms are placed at $z = \frac{3}{8}$ and $-\frac{3}{8}$, just above and below every hexagon in the kagomé net, here the parameters are taken as a fraction of one layer thickness, *i.e.* the kagomé net is sandwiched in-between two triangular nets of Mg atoms. The layer A is different from A' in the atomic position of a small atom at $z = \frac{1}{2}$.

If A and A' are shifted by $\frac{1}{3}$ or $\frac{2}{3}$ to the $[\bar{1}10]$ direction of the hexagonal cell, B and B' or C and C' are

0567-7394/80/010016-06$01.00

obtained, respectively. The layer stacking conforms to the spatial requirements of the atoms, and each layer can only be followed by two particular layers. Possible ways of stacking the layers are shown by arrows in Fig. 2, and c and h sequences (Komura & Kitano, 1977) are also inserted in the figure. The C_{15}(f.c.c.) structure is composed of only the c sequence, while the C_{14}(two-layer) structure consists of the h sequence. A compound layer, say A, can be divided into two parts; one is a triplet which consists of a kagomé net sandwiched in-between two triangular nets, and the other is a remaining triangular net at $z = \frac{1}{2}$. The former part is called α, β or γ, and the latter a, b or c as shown in Fig. 1 (Allen, Delavignette & Amelinckx, 1972). Therefore, layer A consists of α and c. If the notation $A = (\alpha, c)$ is used, the other layers are written as follows; $A' = (\alpha, b)$, $B = (\beta, a)$, $B' = (\beta, c)$, $C = (\gamma, b)$ and $C' = (\gamma, a)$. As Allen, Delavignette & Amelinckx (1972) pointed out, it is assumed that stacking faults will presumably occur between the triplets rather than within the triplet in the Laves phase structure.

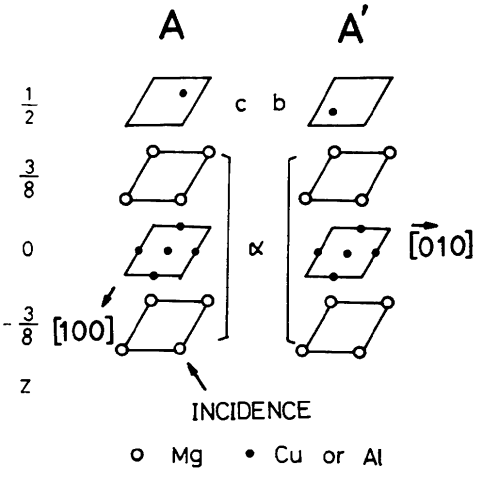

Fig. 1. Two compound layers A and A' of the Friauf–Laves phase. The parameter z is taken as a fraction of the distance between two kagomé nets. A symbol α represents the triplet and symbols b and c the triangular nets.

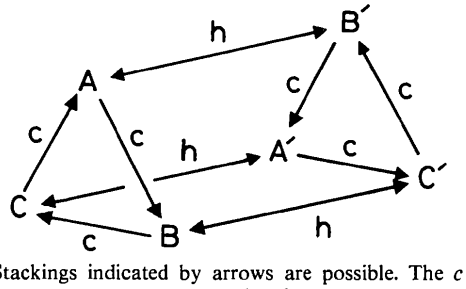

Fig. 2. Stackings indicated by arrows are possible. The c and h sequences are also shown.

Experimental procedure

The prepared composition of the alloys investigated is $Mg(Cu_{1-x}Al_x)_2$ with $x = 0{\cdot}465$. Pure Mg, Cu–Al mother alloy and a necessary amount of pure Cu were melted in an Ar-filled induction furnace. They were vigorously stirred and then cast into a cylindrical graphite mold. All metals used were of grade 99·9%. Ingots were sliced into discs less than 0·2 mm thick. Thin foils were obtained from the discs by electropolishing in a mixed solution of HNO_3 and CH_3OH, and were examined under a JEM 100C electron microscope, operated at 100 kV. They were oriented on a high-resolution goniometer stage so that the [110] direction of the hexagonal cell was aligned parallel to the incident beam. Then we obtained the $\bar{h}hl$ reciprocal net, from which we could easily identify the structure and recognize the features of the stacking faults in the specimen. In this orientation the lattice images were recorded at a magnification of $3{\cdot}2 \times 10^5$ after inserting an objective aperture which restricted the number of diffracted beams to about thirty. In this case, an improvement of the resolution could be achieved by using more diffraction spots such as $00\pm l$ and $\pm 1 \mp 1 \pm l$ compared with the previous work (Kitano, Komura & Kajiwara, 1977), in which only a few $00\pm l$ spots due to multiple diffraction were used.

Results and discussion

(a) *Regular structure*

Two-dimensional lattice images of the two-, four-, and nine-layer type structures are shown in Figs. 3, 4 and 5, respectively. The dimensions of each unit cell are inserted in each figure. The distance between two adjacent white patches in the $[\bar{1}10]$ direction is equal to 4·4 Å, which is half of the period in this direction. These rows of white patches are stacked in the c direction with an interval of 4·2 Å, the thickness of the compound layer. On the right of each image is shown the (110) projection of each structure determined by the single-crystal X-ray method. In the figures, two atomic planes are drawn in full and dotted lines, which are stacked alternately in the [110] direction with an interval of half the period. The atoms shown by small full circles are placed at the center of the two planes. In the projection, large open circles represent Mg atoms and small full and open circles Cu or Al atoms. Basal planes (perpendicular to the c axis) containing the small full circles form the kagomé nets. Comparing the lattice images with the projections, it is easily found that relative shifts of the white patches in the $[\bar{1}10]$ direction correspond to the shifts of kagomé nets. Then the small full circles on the kagomé net in the projection may be thought of as the white patches in the images, though

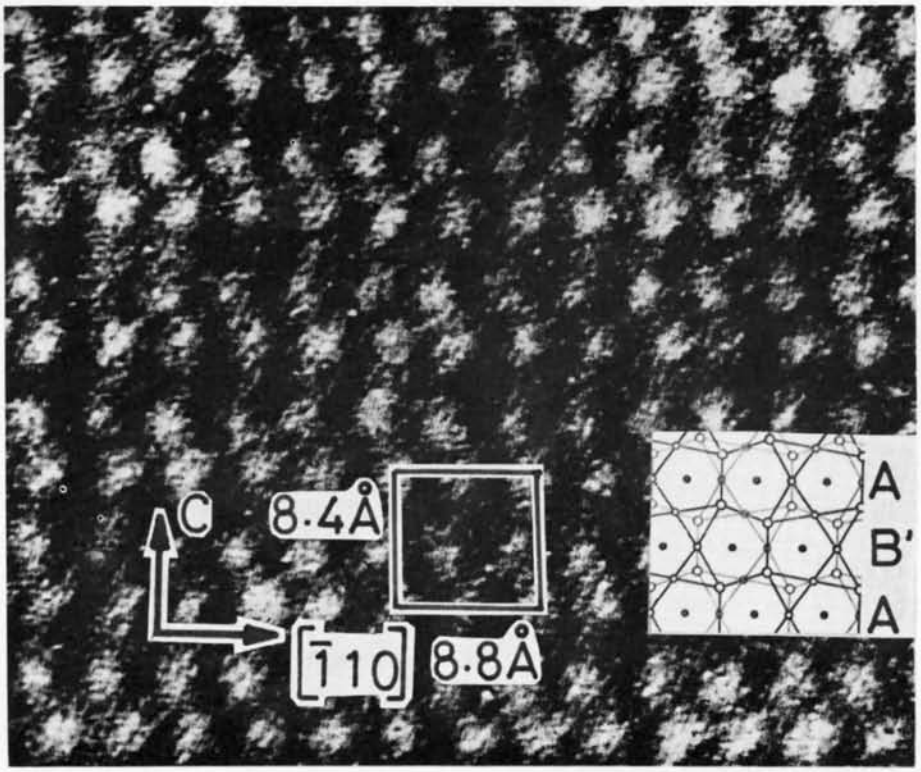

Fig. 3. Lattice image and projection of the two-layer structure (AB').

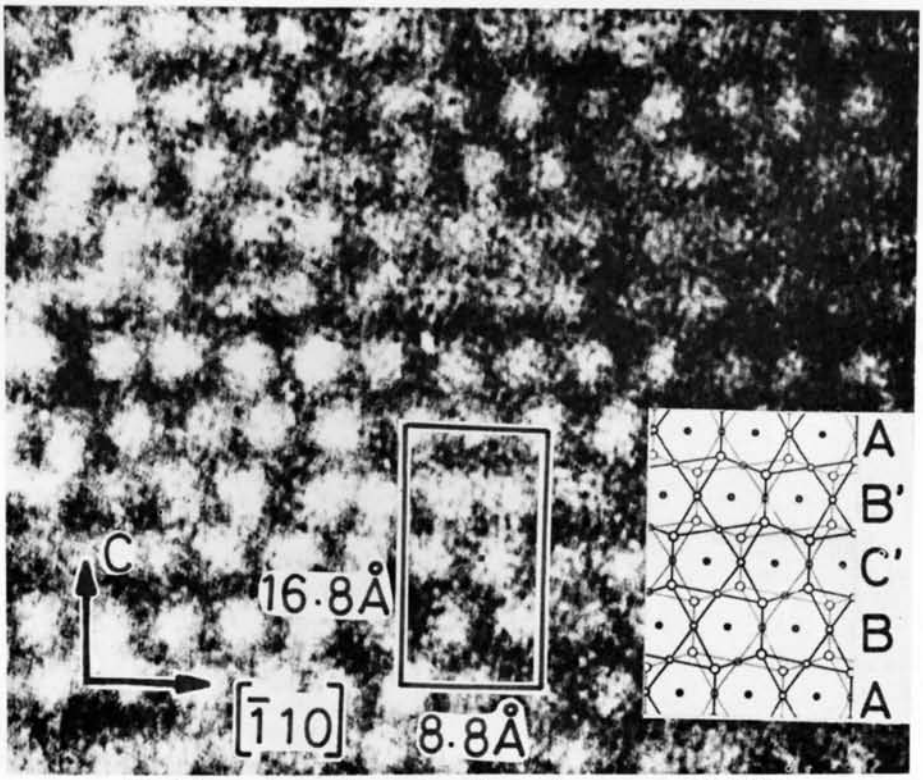

Fig. 4. Lattice image and projection of the four-layer structure ($ABC'B'$).

the interval between the rows of the white patches in the c direction varies somewhat layer by layer, especially in the case of the two-layer structure (Fig. 3). The variation of the interval may be partly due to a small tilt of the specimen with respect to the incident beam. From the shifts of the white patches layer by layer, we can determine the layer stacking sequence with the aid of the ways of stacking the layers in Fig. 2. The stacking sequences thus determined are the same as those determined by X-ray analysis. Thus the direct correlation between the image and the crystal structure was established. The atoms shown as small filled circles on the kagomé net are piled up to give twice as many as the other atoms, marked by the open small and large circles. The white patches in this image correspond to the rather dense parts of the electron cloud in the Laves phase structure.

(*b*) *Disordered stacking sequence*

A two-dimensional lattice image with an irregular stacking sequence is shown in Fig. 6. The layer stacking sequence could be determined from the shifts of the rows of the white patches in the $[\bar{1}10]$ direction. The stacking sequence of more than 200 layers was determined but no regular structure could be found in this region. However, a characteristic feature was observed; successive c sequences and more than four successive h sequences were not observed. This feature is similar to the one which exists in the regular structures of the Mg-based Laves phase found near the electron concentration of the present alloy. In the region on the left-hand side of Fig. 6, the lattice image is clearly two-dimensional but on the right-hand side, where the fragment may be a little thicker, some of the rows of white patches become dull and weak even though others remain sharp and strong. If one assumes that the kind of layer does not change when going from a thin to a thicker region in this image, we can designate the layer stacking sequence even in the thicker region. We may say in this case that every dull and weak row corresponds to a layer with a prime (A', B' or C'), while every sharp and strong one to a layer without a prime (A, B or C).

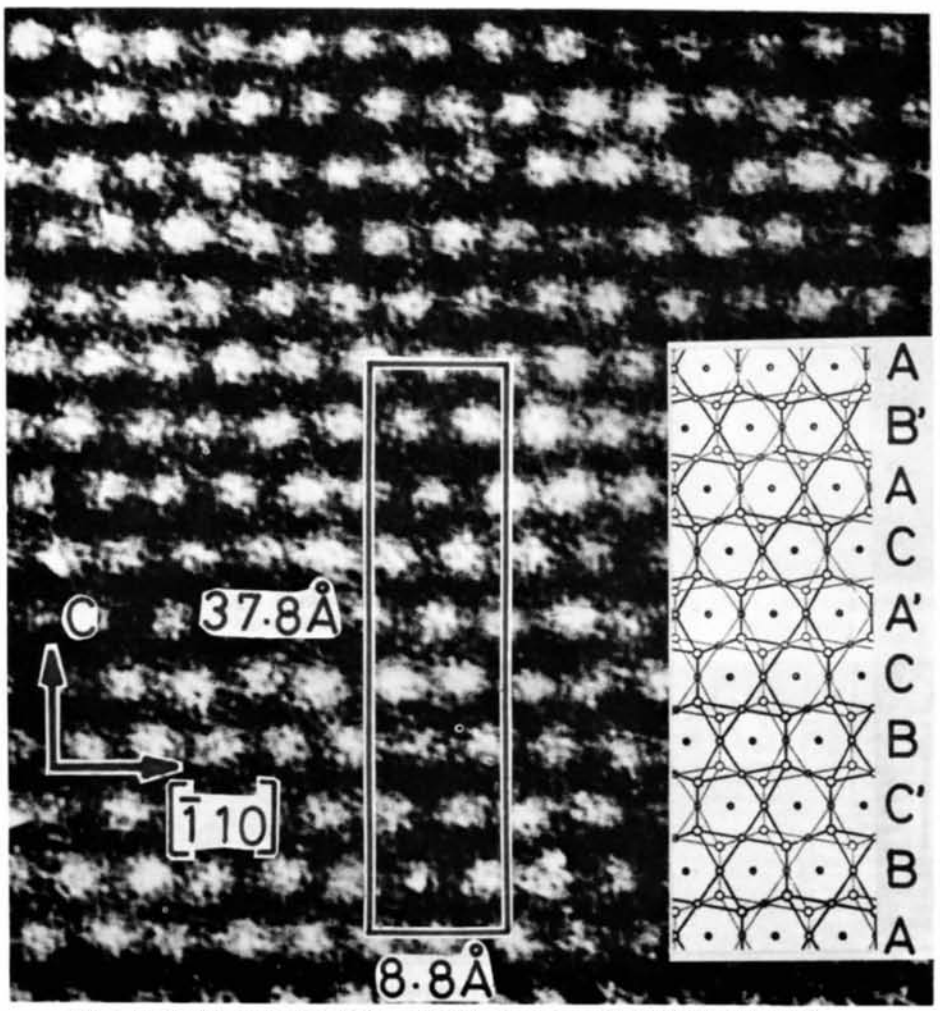

Fig. 5. Lattice image and projection of the nine-layer structure ($ABC'BCA'CAB'$).

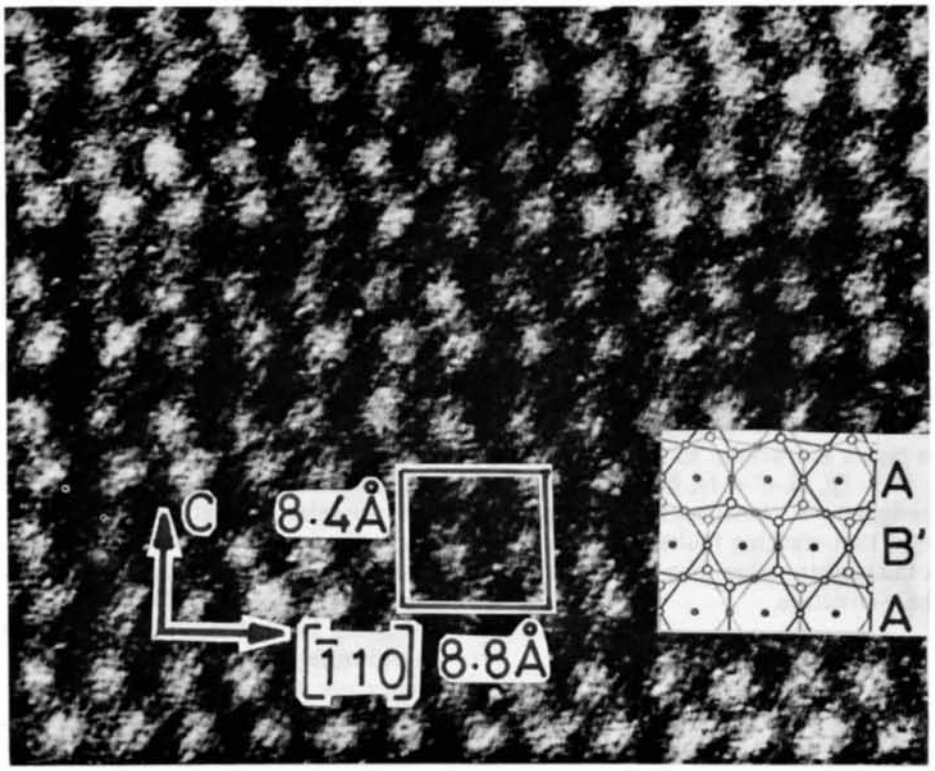

Fig. 3. Lattice image and projection of the two-layer structure (AB').

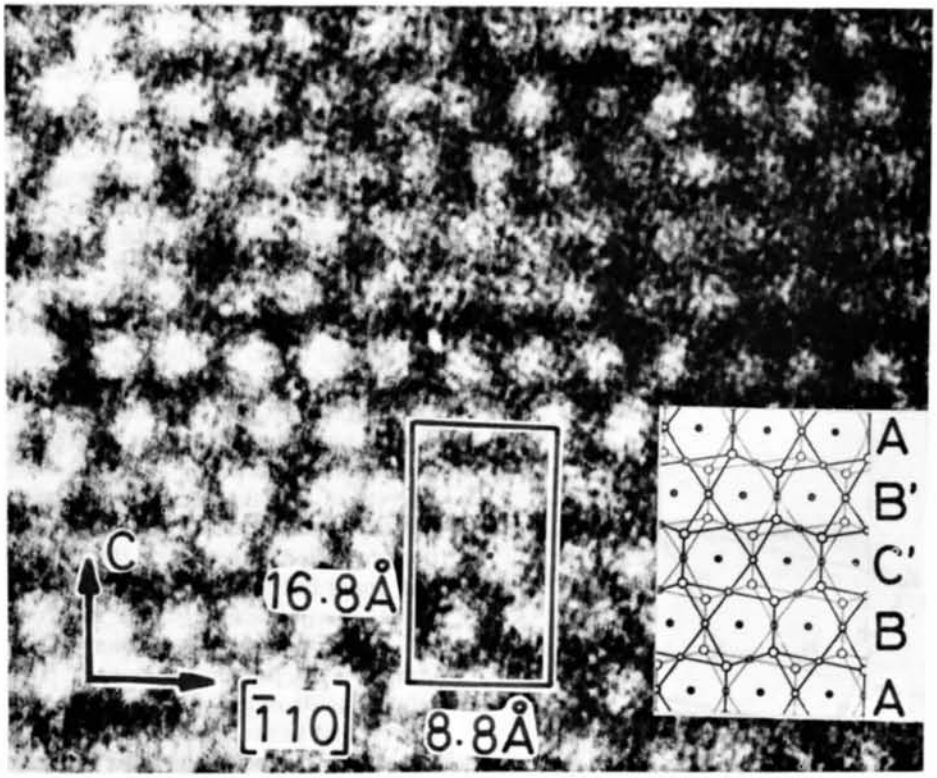

Fig. 4. Lattice image and projection of the four-layer structure ($ABC'B'$).

(*c*) *A new type of defect*

A new type of defect is observed in the lattice images. Examples of the defect are shown in Fig. 7 by roman numerals. From inspection of the figure, it is seen that the lattice is deformed in a very narrow region near the defect, so that the defect can be considered as linear and piercing through the specimen parallel to the incident beam. Since no extra half-plane is found near the defect and no disturbances in the periodicity of the white patches in the [$\bar{1}$10] direction, except for the layer containing the defect, the linear defect is not the usual dislocation which is always surrounded by a strain region.

The linear defects in the figure may be thought of as

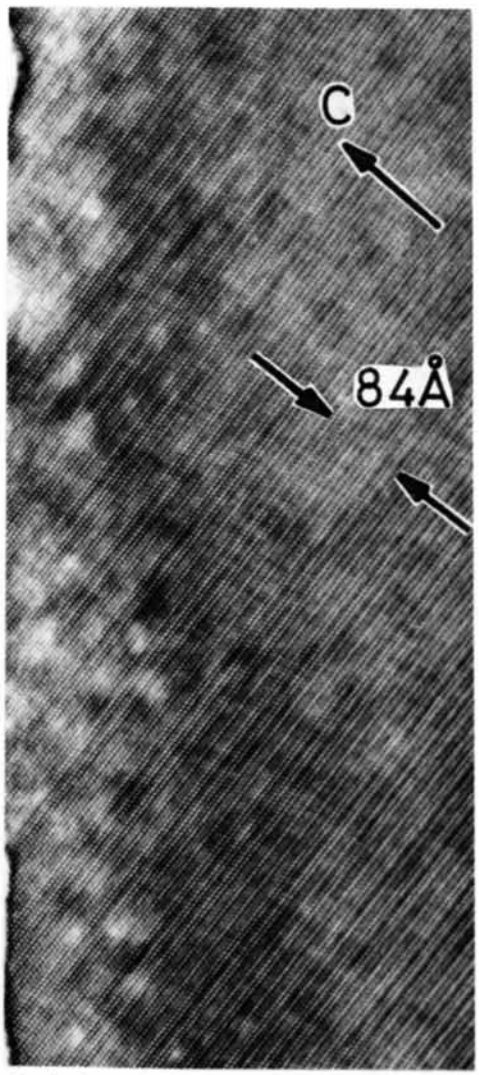

Fig. 6. Lattice image in the region where the stacking sequence is not regular.

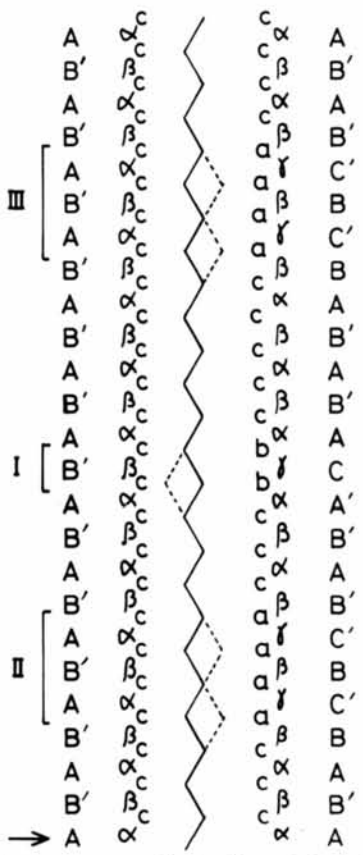

Fig. 8. Stacking sequences of both sides of the defects over the same area as in Fig. 7. An arrow and the defects I, II and III correspond to those of Fig. 7.

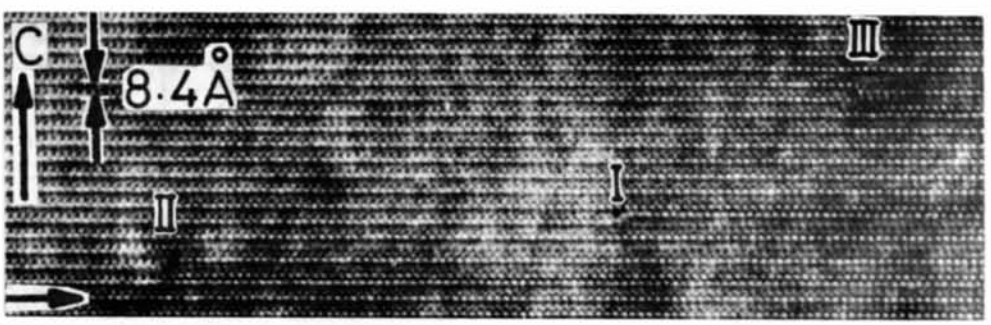

Fig. 7. Lattice image containing a new type of defect in the two-layer structure. The layer marked by a horizontal arrow is assigned to a layer *A*. Defects are shown by I, II and III.

characteristic structural defects in the Laves phase structure. Let a sharp fringe below the defect be assigned to an A layer (shown by a horizontal arrow in the figure), then the layer sequence on each side of the defect can be determined from the image. The layer sequences of both sides of the defects are shown in Fig. 8. The layers are represented in two ways as described before. The zigzag line at the center of Fig. 8 is obtained when the small full circles in the projection are connected layer by layer. This zigzag line is conveniently used since a layer without a prime corresponds to a segment with positive slope and a layer with a prime to negative slope. The dotted parts in the zigzag line correspond to the layers containing the defects. It is found from the figure that an equal number of planes are stacked on each side of the defect and that only a few atomic planes are shifted with respect to the left-hand side of the defect. The shift is characterized by the following two types:

$$\begin{pmatrix} c \to a \\ \alpha \to \gamma \\ c \to a \end{pmatrix} N \text{ type}$$

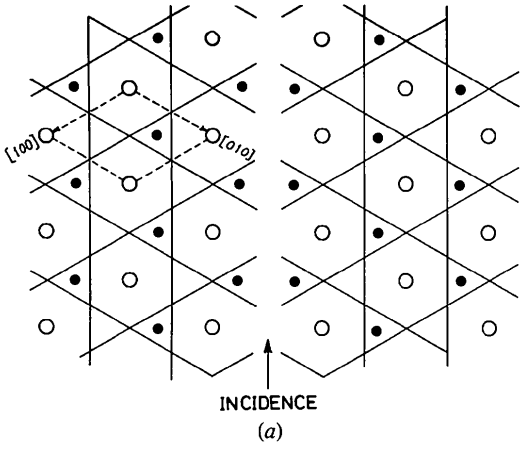

Fig. 9. Models of the atomic arrangement of (001) planes containing the new type of defect; (*a*) *N* type, (*b*) *P* type.

and

$$\begin{pmatrix} c \to b \\ \beta \to \gamma \\ c \to b \end{pmatrix} P \text{ type.}$$

When the letters are changed cyclically ($a \to b \to c \to a$ and $\alpha \to \beta \to \gamma \to \alpha$), an equivalent *N*- or *P*-type defect is produced. Basal planes which contain the defects are illustrated in Fig. 9, in which (*a*) corresponds to the *N* type and (*b*) to the *P* type. In the figures are drawn the atomic configurations at both sides of the defect. The kagomé net and large open circles represent one of the triplets; α, β or γ, and the planes with small full circles are the net planes just above and below the triplet. A defect is formed by two kinds of shifts of an α triplet and two triangular nets in the basal planes. The *N*-type defect consists of a $[\bar{2}\bar{1}0]/3$ shift of an α triplet and $[\bar{1}\bar{2}0]/3$ shifts of two *c* planes which are just above and below the α triplet. The *P*-type defect consists of a $[\bar{1}\bar{2}0]/3$ shift of a β triplet and $[\bar{2}\bar{1}0]/3$ shifts of two *c* planes. The shifted net planes are sandwiched in-between two β triplets in the *N* type or two α triplets in the *P* type. The planes above and below the faults are not affected by the shifts at all. This structural defect is one of the simplest ones causing a stacking fault in the Friauf–Laves phase. The stacking fault caused by this defect can be represented as follows; in the *N* type the stacking order of the layers changes from $AB'A\underline{B'}AB'AB'$ to $AB'A\underline{BC}'B'AB'$, and in the *P* type from $AB'\underline{AB}'AB'AB'$ to $AB'\underline{A'C}AB'AB'$. Only the underlined parts are changed, and other parts are not affected. The defects indicated by II and III in Figs. 7 and 8 are examples of successive such defects. The deformed area around these defects becomes a little larger than the single defect (I). Both types of defect (*N* and *P*) are observed in the photograph at the same time in Fig. 7. Similar types of defects were also observed in lattice images of the four- and nine-layer structures. In all cases, the defect occurred at an *h* sequence.

The authors wish to thank Mr M. Mitarai and Mr K. Tokunaga of Hiroshima University for preparing the alloy specimens. This work was partly supported by the Grant-in-Aid for Scientific Research from the Ministry of Education, to which the authors' thanks are due.

References

ALLEN, C. W., DELAVIGNETTE, P. & AMELINCKX, S. (1972). *Phys. Status Solidi A*, **9**, 237–246.

FRANK, F. C. & KASPER, J. S. (1959). *Acta Cryst.* **12**, 483–499.

KITANO, Y., KOMURA, Y. & KAJIWARA, H. (1977). *Trans. Jpn Inst. Met.* **18**, 39–45.

KOMURA, Y. (1962). *Acta Cryst.* **15**, 770–778.

KOMURA, Y. & KITANO, Y. (1977). *Acta Cryst.* B**33**, 2496–2501.

KOMURA, Y., MITARAI, M., NAKATANI, I., IBA, H. & SHIMIZU, T. (1970). *Acta Cryst.* B**26**, 666–668.

KOMURA, Y., MITARAI, M., NAKAUE, A. & TSUJIMOTO, S. (1972). *Acta Cryst.* B**28**, 976–978.